Ecological Engineering 158 (2020) 106065

Contents lists available at ScienceDirect

Ecological Engineering

journal homepage: www.elsevier.com/locate/ecoleng

Removal of nitrogen from rainwater runoff by bioretention cells filled with modified collapsible loess

Jiaqing Xiong[a,b,*], Jiajia Zhou[a,b], Jianqiang Li[a,b], Guoqing Sun[a,b], Xiaochang C. Wang[a,b], Shengxia An[c], Wanqin Li[c], Jie Wang[a,b]

[a] Key Lab of Northwest Water Resource, Environment and Ecology, MOE, Xi'an University of Architecture and Technology, Xi'an 710055, China
[b] School of Environmental and Municipal Engineering, Xi'an University of Architecture and Technology, Yan Ta Road. No.13, Xi'an 710055, China
[c] Qinghai Building and Materials Research Academy Co., Ltd, No. 6, Jianyan Lane, Wusi West Road, Xining City 8 10008, China

ARTICLE INFO

Keywords:
Collapsible loess
Bioretention cell
Rainwater runoff
Nitrogen

ABSTRACT

The construction of bioretention facilities in collapsible loess areas faces some problems such as low infiltration rate of rainwater runoff and system blockage, which seriously affect the treatment effect of bioretention cell on rainwater runoff. According to the different filler matrix, three bioretention cells with improved filler were constructed, the 1# bioretention system was filled with 50% of the construction waste mixed with 50% loess, and the 2# bioretention system was filled with 50% concrete sand mixed with 50% loess, the 3# bioretention system was filled with 45% concrete sand +10% wood chips +45% loess mixed in the bioretention cell. The results show that the removal rate of NH_4^+-N is the highest when the height of the inundation zone of the bioretention cell is 600 mm (more than 98%). The change of hydraulic load and submerged zone height had a significant effect on the removal rate of NO_3^--N in bioretention cell ($P < 0.05$). The removal rate of NO_3^--N in the bioretention cell decreased with the increase of hydraulic load, and the bioretention cell had the highest removal rate of NO_3^--N (48.85%) under low hydraulic load conditions. The removal rate of NO_3^--N in the bioretention cell increased with the increase of the height of the inundation area, and the removal rate of NO_3^--N was the highest when the inundation area height of the bioretention cell was set at 600 mm (98.33%). The improved bioretention cell has a better effect on NH_4^+-N treatment during the wet period, and the NH_4^+-N concentration of the effluent is below 0.4 mg/L. The NO_3^--N concentration in the effluent of the three improved bioretention cells during the wet period differed greatly. Among them, the bioretention cells using sawdust modified fillers had the highest removal rate of NO_3^--N. The collapse amount of the three improved bioretention cells was below 0.5 cm, and the permeability coefficients were above 2 cm/h. The experiment proves that the three methods to improve the collapsible loess filler can be applied to the construction of the bioretention cell in the collapsible loess area so that the bioretention technology can be effectively promoted in the loess area. This experiment has great significance to the construction of bioretention cells in the loess area.

1. Introduction

With the rapid development of urban construction, the original natural water bodies and green spaces have gradually disappeared (Shrestha et al., 2018). Urban development has greatly increased the impervious area of the city, making it difficult for rainwater to infiltrate, which has led to a substantial increase in flood peak flow and rainwater runoff (Mahmoud et al., 2019). Also, the transportation of pollutants and nutrients in surface runoff leads to serious water pollution (Fan et al., 2019). Related studies showed that more than 50% of nitrogen pollution in rivers, lakes, and oceans come from stormwater runoff (Davidson et al., 2009; Gao et al., 2019).

Bioretention cell is an optimal management facility for rainwater, which is widely used to solve urban flooding and stormwater runoff pollution (LeFevre et al., 2015; Wang et al., 2019). Collapsible loess is widespread throughout the world, including Asia, Africa, Central and Southern Europe, Antarctica, the Northwest, and the Central United States, Northern Russia, Alaska Inland and South America (such as Argentina), and other regions (Roberts et al., 2013). For collapsible loess, most of the researches are on the optimization of collapsibility and bearing capacity (Liu and Shen, 2009; Zhirong, 2019). There are few studies on the removal of pollutants by collapsible loess. Still, some

* Corresponding author at: Key Lab of Northwest Water Resource, Environment and Ecology, MOE, Xi'an University of Architecture and Technology, Xi'an 710055, China.
E-mail address: xiongjiaqing@xauat.edu.cn (J. Xiong).

https://doi.org/10.1016/j.ecoleng.2020.106065
Received 17 February 2020; Received in revised form 7 September 2020; Accepted 21 September 2020

studies have proved that the red soil has a good removal effect on pollutants, and the removal rates of ammonia nitrogen and total phosphorus are more than 80%. Therefore, the feasibility of using collapsible loess as bioretention cells can be considered. Loess is mainly composed of quartz, feldspar and water-soluble salt. Water-soluble salt is one of the causes of loess collapsibility. It can produce cementation when it is attached to the surface of particles. After meeting water, the salt dissolves, and the cementation disappears. And then cause loess collapsibility (Wan-Li et al., 2015). Also, loess is formed by sediment and clay particles under the action of aeolian formation (Liu et al., 2015). When the loess is infiltrated with water, the loess particles are hydrated. During the hydration process, the clay coating is separated from the slime particles, which will cause the soil structure to collapse (Sadeghi et al., 2019). The collapse of soil structure mainly affects its mechanical properties and hydraulic properties. Soil collapse causes a decrease in the number of large and medium voids in the soil, leading to a decrease in soil porosity (Zhang et al., 2019). The decrease in soil porosity will reduce the permeability of the seepage area of the bioretention cell, which will easily cause problems such as blockage of the bioretention cell and low purification efficiency, and affect the service life of the system. To improve the water permeability of the bioretention cell in the collapsible loess area, extend the service life of the bioretention cell, and achieve the purpose of removing NH_4^+-N and NO_3^--N from the rainwater runoff, it is necessary to modify the collapsible loess filler.

The infiltration effect of the bioretention system using the collapsible loess as the substrate does not meet the target requirements of stormwater runoff control and treatment. The methods for modifying collapsible loess in the site mainly include dynamic compaction method (also called dynamic consolidation method) and chemical improvement method. The dynamic compaction method can better improve the mechanical and hydraulic properties of the soil, and often has a strong filling and compacting effect, which easily causes the reduction of large pores in the filler, thus affecting the effect of water infiltration and water retention (Jing et al., 2014; Peng et al., 2017). Chemical improvement is a method of adding other substances to the soil to improve the gradation and organization of soil particles. In addition to the commonly used wood chips, coarse sand, crushed stone, lime, cement and fly ash , new materials such as polymer and composite water glass can be added to improve soil permeability (Zheng-Zheng and Gao, 2018). The effects are of different additive materials on the porosity of the filler is significantly different. The study showed that after a period of maintenance, the permeability coefficients of compacted soil, a certain proportion of lime soil, cement soil, etc. are weakened, while the certain proportion of lime soil (lime and fly ash loess) has very good permeability; this indicated that the undisturbed loess could be improved in a certain way to maintain the stable permeability of the loess and solve the collapsibility problem (Hai-Zhen and Yang, 2011). These research results based on the safety control of collapsibility suggested that the soil collapsibility is eliminated through soil chemical improvement while maintaining the water permeability and water holding capacity of the matrix, and it can maintain stability for a long time. In addition to permeability, the nature of the filler also has an important effect on the purification of rainwater. Tang et al. (2016) monitoring and analyzing of two years of biological retention facilities with sand, soil layering and homogeneous loess, soil stratification and homogeneous loess bioretention facilities; this showed that the stratified packing had higher peak runoff reduction and water reduction than homogeneous loess filler, but the difference is not obvious in purification effect. These studies that the modification of collapsible loess does not only ensure the safety of the structure of the facility, but also maintains a certain permeability and the modification measures adopted have a good purification effect against stormwater runoff pollution. Therefore, it is necessary to study what kind of filler and collapsible loess is used to fill the bioretention cells, which can reduce the blockage and effectively remove pollutants. In this experiment, the treatment effect of bioretention cells was demonstrated by analyzing the variation of nitrogen concentration in effluent and influent. However, there is no further study on the nitrogen cycle in the system, which can be used as the future research direction.

Three different modified bioretention cells were designed in this study. The hydraulic performance and the removal efficiency of pollutants in rainwater runoff on improved bioretention cells were studied. In this experiment, bioretention cells with different packing combinations have been constructed. Under the same influent conditions, the effluent NH_4^+-N and NO_3^-N concentrations were compared, and the optimal packing combination has been found by analyzing the data. The purpose of this experiment is as follows: (1) the operation status of bioretention cells are improved in the loess area by mixing other fillers with loess. (2) blockage is avoided. (3) the removal effect of pollutant is improved. (4) based on not changing the original soil, the bioretention cells are constructed to reduce the cost.

2. Materials and methods

2.1. Improved stability and permeability of fillers

Four measuring cylinders with an inner diameter of 95 mm were set in the laboratory and filled with a modified loess filler with a height of 450 mm. The specific filler ratio is shown in Table 1. The top of the improved loess filler was covered with a small amount of gravel to prevent the surface soil from being washed. The inner wall of the cylinder was sanded with coarse sandpaper and pre-coated with fine sand to prevent short-flow. 1 L of water was injected from the top of the experimental device, and the surface sedimentation was detected while measuring the permeability coefficient of the filter medium.

2.2. Construction of bioretention cell

Three bioretention cells were constructed in a sewage treatment plant in Xi'an, Shaanxi Province, as shown in Fig. 1. Briefly, the bioretention cell was constructed by mounting filter media and perforated tubes in three HDPE cylindrical vessels (25 cm diameter × 122 cm height), as shown in Fig. 1. The bottom of each cylindrical container was filled with 20 cm deep gravel (d50 = 4.75 cm) as a drainage layer, and 2 cm (inner diameter 4.75 cm outer diameter 5 cm) drain pipe was set from the bottom of the drainage layer, and a spherical valve was set. A drain standpipe (inner diameter 2.7 cm outer diameter 3 cm) was added to the outlet of the drainpipe, and a spherical valve was placed every 15 cm on the standpipe. Filling the seepage area of the bioretention cell with construction waste (diameter 3 mm-5 mm), concrete sand (directly 1 mm-2 mm), wood chips (diameter 5 mm-10 mm) mixed loess (direct diameter 0.15 mm-0.35 mm). Gravel (d50 = 4.25 mm) was filled as a cover layer above the bioretention cell. Biologically inoculate the bioretention cell, and diluted the 500 mg/L activated sludge solution in dechlorination tap water at 8000 mg/L activated sludge (Siyuan Wastewater Treatment Plant) and added it to each bioretention cell until the water was observed at the drain (Tian et al., 2019).

In the seepage area of the bioretention cell, the loess was mixed with construction waste, concrete sand and wood chips to fill the bioretention cell with a packing height of 80 cm. In the three kinds of bioretention cells, the 1# bioretention system was filled with 50% of

Table 1
Modified filler formula.

Code	Filler
HT	100%loess
JT	50%Construction waste + 50%loess
ST	50%Sand + 50%loess
STM	45%Sand + 10%Chip + 45%loess

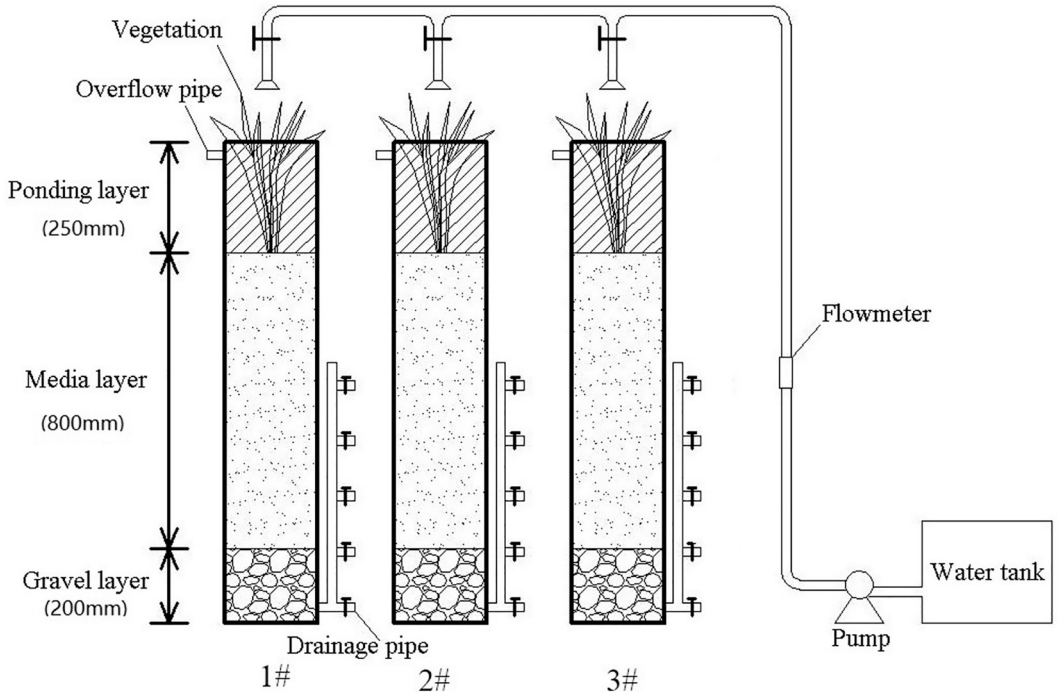

Fig. 1. Shows the bioretention cell device. The 1# infiltration zone packing is 50% of construction waste and 50% of loess mixed; the 2# seepage zone packing is 50% concrete sand and 50% loess mixed; 3# seepage zone packing is 45% concrete sand, 45% loess and 10% wood chips are mixed.

Table 2
Physical and chemical properties of the filler in the seepage zone of the bioretention cell.[a, b]

Composition (v/v)	1#	2#	3#
	50%Construction waste + 50%loess	50%Sand + 50%loess	45%Sand + 10%Chip + 45%loess
Depth (cm)	80	80	80
Volume (L)	40	40	40
Dry mass (kg)	62 ± 5	66 ± 5	62.6 ± 5
Bulk density (g/cm3)[c]	1.55 ± 0.01	1.65 ± 0.01	1.565 ± 0.01
Estimated total porosity (v/v)[c]	0.58 ± 0.01	0.27 ± 0.01	0.32 ± 0.01
Estimated pore volume (L)[c]	23.2 ± 0.4	10.8 ± 0.4	12.8 ± 0.4
d50 (mm)[c]	0.95	0.42	0.45
pH (1:1)[c]	7.78 ± 0.05	5.02 ± 0.06	6.13 ± 0.02

[a] Twenty centimetres of loess and sixty centimetres of building waste are layered.
[b] " ± " represents one standard error of the mean.
[c] Particle size analysis followed ASTM D422-63; pH followed ASTM D4972-13; organic matter followed ASTM D2974-13. Total porosity measured in the lab using packed filter medium columns with identical bulk densities to media in field; Pore volume is product of total porosity and the zone volume.

the construction waste mixed with 50% loess, and the 2# bioretention system was filled with 50% concrete sand mixed with 50% loess, the 3# bioretention system was filled with 45% concrete sand +10% wood chips +45% loess mixed in the bioretention cell. The filler material in the mixed filler in the percolation zone is a volume ratio. The physical and chemical properties of the fillers in each bioretention cell are shown in Table 2. A geotextile was laid at the junction of the seepage zone and the drainage layer. *Ophiopogon japonicus* (80 strains/m^2) are planted in three improved bioretention cells (Mahmoud et al., 2019).

2.3. Simulated rainwater runoff experiment

The removal rate of NH_4^+-N and NO_3^--N in the modified bioretention cells was evaluated by three different conditions of infiltration experiments. The influent water quality was configured according to the road rainwater runoff pollutants in Xi'an, see Table 3. The first infiltration experiment was carried out under the conditions of low hydraulic load (20.04 mL/min), medium hydraulic load (30.37 mL/min) and high hydraulic load (37.74 mL/min) through the water cell and peristaltic pump water distribution. The rainwater runoff experiment was run for six days under each hydraulic load, and the water was injected for 8 h every day. After each change of the hydraulic load, the water is stabilized for three days before the next hydraulic load test. The collected water sample was filtered through a 0.45 μm filter to detect the concentration of NH_4^+-N and NO_3^--N.

Table 3
simulates surface runoff water quality configuration.

Contaminant	Chemical reagent	Concentration (mg/L)
NO_3^--N	KNO_3	8
NH_4^+-N	NH_4Cl	8
COD	$C_6H_{12}O_6$	300

In the second infiltration experiment, the submerged heights were set to 0 mm, 300 mm, 600 mm for water distribution, the water intake was 30.37 mL/min. The water was supplied for 6 days in each experimental condition, and water was supplied for 8 h each day. At the same time, concentrations of NH_4^+-N and NO_3^--N were detected in the

water.

The submersion height in the third infiltration experiment was 600 mm. According to the 30-year rainfall data of Xi'an, the infiltration duration was set to 3 days, 3 days, 10 days, and 5 days, respectively. After each infiltration, the drought was 5 days, 10 days, 5 days, and the infiltration flow rate was 30.37 mL/min, the infiltration was 8 h per day. The effluent water samples from the bioretention cell were collected to determine the concentrations of NH_4^+-N and NO_3^--N.

2.4. Analysis methods

Considering that most of the loess particles are silt particles, the variable head method was selected for determination (Anping and Yuming, 2019). Referring to the calculation method of permeability coefficient of variable head infiltration test in "Standard for Geotechnical Test Methods" (GB T50123-1999), the Darcy theorem was used to calculate the vertical permeability coefficient of each experimental column. The surface settlement of the filler was measured with a ruler. The concentration of NO_3^--N was determined by ultraviolet spectrophotometry. The concentration of NH_4^+-N was determined by Nessler's reagent spectrophotometry.

2.5. Data processing

Data analysis and processing were performed using Origin 8.5 and SPSS 22.0. One-way ANOVA module was used to analyze the influence of different hydraulic load and inundation area height on the effluent quality of each bioretention cell ($P = 0.05$), and analyze the difference of the influence of different bioretention cells on the effluent quality ($P = 0.05$). The removal efficiency of nitrogen is.

$$R = \left(1 - \frac{C_{ef}}{C_{in}}\right) \times 100\% \quad (1)$$

where R is the removal efficiency (%) of nitrogen, C_{in} and C_{ef} are the concentrations of dissolved nitrogen (mg/L) in the influent and effluent, respectively.

3. Results and discussion

3.1. Improved packing stability and permeability

The results of the settlement of the filler produced by the modified collapsible loess and the unmodified collapsible loess bioretention cell in different water seepage are shown in Fig. 2. It can be seen from the experimental results that in the aspect of soil surface sedimentation, the SMT modified loess mixed with crushed wood chips has the smallest settlement, which is related to the swelling of the wood chips after water absorption. The settlement of HT has increased sharply with the increase of water seepage and then stabilized. The SMT modified loess mixed with crushed wood chips has the smallest settlement, which is related to the swelling of the wood chips after water absorption. The settlement of JT, ST and SMT is small and almost constant, the maximum settlement was 0.5 cm, which may be due to the stable chemical and physical properties of construction waste, concrete sand, and wood chips. After mixing with the loess in proportion, the gradation of the original loess is optimized to form a stable soil - gravel mixes the skeleton, so the settlement is small. The settlement of HT reached 2.7 cm, which was mainly due to the hydration of the loess particles. The hydration causes the loess granular system to be destroyed, resulting in the collapse of the loess filler. The stable settlement values of HT, JT, ST, and SMT are shown in Table 4.

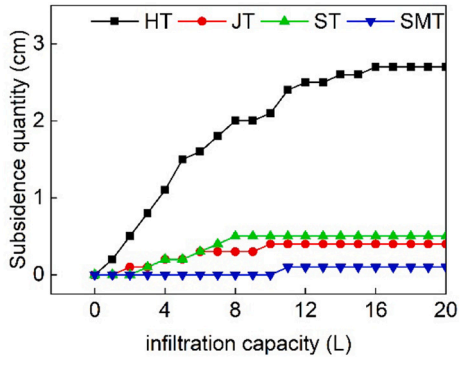

Fig. 2. The amount of collapse under different water seepage. HT is 100% loess filled; JT is 50% construction waste mixed with 50% loess filling; ST is 50% concrete sand mixed with 50% loess filling; SMT is 45% concrete sand mixed with 45% loess and 10% wood chip filling.

The permeability coefficient under different water seepage is shown in Fig. 3. It can be seen from the experimental results that the permeability coefficient of loess under each improved method decreases with the increase of water seepage and tends to be stable. Among them, the permeability coefficient of JT and SMT fluctuated greatly. The permeability coefficient of loess under different improvement schemes was SMT > JT > ST > HT. It can be seen from JT and ST that the addition of construction waste improves the permeability of loess better than the addition of concrete sand, which is related to the large porosity of construction waste. The permeability coefficient of HT was stable at 0.64 cm/h, which was mainly due to the decrease of loess porosity and the decrease of permeation rate after the loess collapses with water. The permeability coefficients of loess in JT, ST, and SMT modified modes were all above 2 cm/h. The permeability coefficient of modified filler is much higher than that of loess filler. This is mainly due to the formation of soil-gravel stabilized aggregate. The porosity of the filler in the improved bioretention cell does not decrease with the increase of the amount of infiltration water, thereby maintaining the permeability of the filler. The permeability coefficient of the modified filler satisfies the requirement of the US EPA of a permeability coefficient of about 1.5 cm/h. It can be selected as a filler for the subsequent bioretention reactor. The permeability coefficient of the unmodified filler is less than 1.5 cm/h and cannot be directly used for the bioretention cell packing. Therefore, only three modified filler bioretention cells were studied in the follow-up study.

3.2. Influence of hydraulic load change on the removal of NH_4^+-N and NO_3^--N in each bioretention cell

The experimental conditions were non-submerged area, and the concentrations of nitrate nitrogen and NH_4^+-N in the inflow were 8.59 ± 0.22 mg/L and 8.53 ± 0.45 mg/L, respectively. Under different hydraulic loads (20.04 mL/min, 30.37 mL/min, 37.74 mL/min), the concentration of N (NH_4^+-N, NO_3^--N) in the effluent of each bioretention cell are shown in Table 5, and the removal rate of N (NH_4^+-N, NO_3^--N) is shown in Fig. 4.

As shown in Fig. 4(a), there is no significant difference in the removal rate of NH_4^+-N between the bioretention cells ($P > 0.05$), indicating that the influent hydraulic load does not affect the removal of NH_4^+-N in the bioretention cell under the experimental conditions. Under high hydraulic load, 2# had the highest removal rate of NH_4^+-N (97.62%), and 1# had the lowest removal rate of NH_4^+-N (94.21%). Under each hydraulic load, the removal rate of NH_4^+-N by 2# is always the highest, and the removal rate of NH_4^+-N by each improved system is relatively high (up to 94.21%). Theoretically, the soil colloid is negatively charged, so it has a positive effect on the positively charged NH_4^+-N. At the same time, the construction waste NH_4^+-N in the packing layer also has adsorption (Jinhui et al., 2017). The NH_4^+-N absorbed by construction waste is reacted into NO_3^--N through nitrification of nitrite bacteria and nitrifying bacteria. Another portion of NH_4^+-N is removed by plant roots and is involved in nitrogen assimilation. However, it generally does not exceed 15% of total removal

Table 4
Stable collapse and permeability coefficient of each filler.

Composition (v/v)	HT	JT	ST	SMT
	100%loess	50%Construction waste + 50%loess	50%Sand + 50%loess	45%Sand + 10%Chip + 45%loess
Filtration coefficient (cm/h)	0.64	4.15	2.46	3.18
Subsidence quantity (cm)	2.7	0.4	0.5	0.1

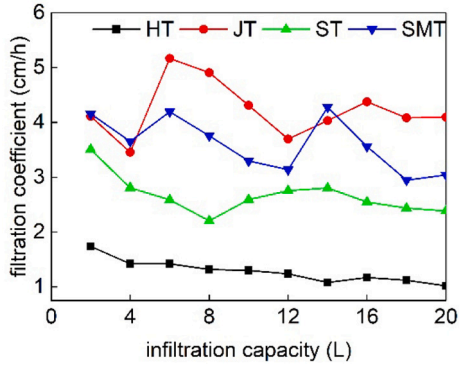

Fig. 3. Permeability coefficient under different water seepage. HT is 100% loess filled; JT is 50% construction waste mixed with 50% loess filling; ST is 50% concrete sand mixed with 50% loess filling; SMT is 45% concrete sand mixed with 45% loess and 10 % wood chip filling.

(Wei et al., 2010).

As shown in Fig. 4(b), with the increase of hydraulic load, the removal rate of NO_3^--N decreased in each bioretention cell, and the change of hydraulic load had a significant difference in the removal rate of NO_3^--N in each bioretention cell ($P < 0.05$). This indicates that the change of urban runoff water volume is an important factor affecting the NO_3^--N removal rate of the three bioretention cells. For 1#, the removal rate of NO_3^--N was negative even under high load, and 2# had the highest removal rate of NO_3^--N compared with other bioretention cells, and the highest (48.85%) under low hydraulic load. The reason why the removal rate of NO_3^--N decreases with the increase of hydraulic load may be that the increase of hydraulic load leads to the increase of the water retention depth of the bioretention cell. The increase in the stagnant water depth of the bioretention cell leads to an increase in the water pressure at the upper part of the facility, which leads to an increase in the infiltration velocity of the water stream, which shortens the hydraulic retention time inside the facility (Table 6). Shortening of the hydraulic retention time leads to insufficient NO_3^--N denitrification in the bioretention cell, and NO_3^--N cannot be removed in the form of N_2 so that the NO_3^--N removal rate is low.

3.3. Influence of the height of the submerged zone on the removal of dissolved N in the bioretention cell

Under the three levels of inundation height (0 mm, 300 mm, 600 mm), the concentration of NO_3^--N in the influent was 8.53 ± 0.69 mg/L, and the concentration of NH_4^+-N was 8.46 ± 0.20 mg/L. The concentrations of NH_4^+-N and NO_3^--N in the effluent of the bioretention cell are shown in Table 7. The removal rates of NH_4^+-N and NO_3^--N at each submerged height of each bioretention cell are shown in Fig. 5.

As shown in Fig. 5(a), The removal rate of NH_4^+-N is generally high, which is directly related to the use of collapsible loess as the filler. The soil is negatively charged and can adsorb NH_4^+-N. However, the bioretention cells with collapsible loess as the filler is easy to block and collapse. Adding construction waste, concrete sand and wood chips into collapsible loess can not only avoid these situations but also increase the contact area between rainwater and filler. Also, the adsorption properties of construction waste and concrete sand also have a certain effect on the removal of NH_4^+-N. In this experiment, the height change of the submerged area was significantly different from the NH_4^+-N effluent concentration of 1# and 3# ($P < 0.05$). The altitude changing of the submerged area had no significant difference with the NH_4^+-N effluent concentration of 2# ($P > 0.05$). The removal rate of NH_4^+-N in the three bioretention cells of 1#, 2#, 3# in the inundation area was increased from 94.62%, 97.04%, 95.94% in the non-submerged area to 98.79%, 98.51%, 98.61%, so in to increase the removal rate of NH_4^+-N, the submergence height can be set at about 600 mm. When the submerged zone was set, the hydraulic retention time became longer (Table 8), which provided sufficient time for the substrate adsorption or ion exchange to remove the NH_4^+-N process. When the submerged height was 300 mm, the removal rate of 1# to NH_4^+-N was lower than that of the non-submerged area, and it was improved when the height of the submerged area was 600 mm. The possible reason is that when the submerged height was 300 mm, the influent NH_4^+-N was converted into NO_3^--N by nitrification in the upper aerobic zone, and was transformed and utilized by the microorganism together with NO_3^--N in the influent water. The removal of NO_3^--N by microorganisms mainly depends on the dissimilatory reduction of microbial nitrate and the nitrogen assimilation of plants. The dissimilatory nitrate reduction includes denitrification and nitrate dissimilation to ammonium (DNRA) (Kellogg et al., 2010). Under the condition of the submerged height of 300 mm, some NO_3^--N acted as electron acceptors under the action of nitrate reductase and nitrite reductase, and the DNRA process was reduced to NH_4^+-N, resulting in a high concentration of 1# effluent NH_4^+-N. The NH_4^+-N removal rate decreased. Under the conditions of 600 mm submerged height, the same anaerobic, high concentration of electron acceptor NO_3^--N, and high COD content of the organic substrate, the denitrification process is only transferred by converting 1 electron per 1 M of nitrate in the DNRA process. The transfer of 5 electrons 30 results in denitrification stronger than DNRA, and most of the NH_4^+-N adsorbed by the matrix is removed by Nitration and Denitrification to N_2 (O'Reilly et al., 2012).

As shown in Fig. 5(b), the setting of the submerged zone can

Table 5
Concentration of effluent N in effluent.

Hydraulic loading	NH_4^+-N (mg/L)			NO_3^--N (mg/L)		
	1#	2#	3#	1#	2#	3#
Low	0.43 ± 0.10	0.29 ± 0.10	0.33 ± 0.07	6.73 ± 0.29	4.39 ± 0.43	4.86 ± 0.52
Middle	0.46 ± 0.07	0.25 ± 0.06	0.35 ± 0.13	7.83 ± 0.46	5.26 ± 0.43	5.84 ± 0.54
High	0.49 ± 0.06	0.20 ± 0.06	0.34 ± 0.05	8.60 ± 0.57	5.57 ± 0.19	6.08 ± 0.30

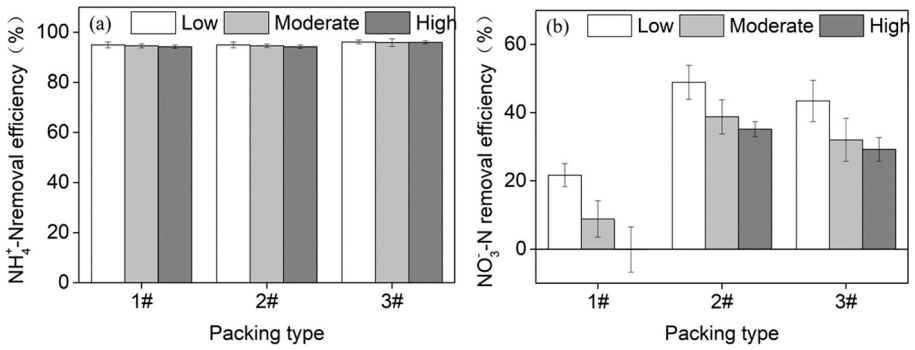

Fig. 4. Removal rates of (a) NH_4^+-N and (b) NO_3^--N under three hydraulic loads. Low stands for the low hydraulic load (20.04ml/min); moderate stands for the medium hydraulic load (30.37ml/min); the high stands for high hydraulic load (37.74ml/min).

Table 6
The hydraulic retention time of different hydraulic loads in each bioretention cells.

Hydraulic loading	The hydraulic retention time		
	1#	2#	3#
Low	10 h	11 h	13 h
Middle	6 h	8 h	9 h
High	5 h	6 h	7 h

significantly increase the removal rate of NO_3^--N in each system ($P < 0.05$). When the submerged zone was not set, the highest removal rate of NO_3^--N was 38.69%, and the highest removal rate of NO_3^--N was 98.33% when the height of the submerged zone was 600 mm. The removal rates of NO_3^--N in the three bioretention cells of 1#, 2#, and 3# increased from 8.70%, 38.69%, and 31.93% in the non-submerged area to 51.11% and 98.33%, 92.72%. It can also be seen from Fig. 5(b) that the addition of wood chips as a carbon source to provide electrons for the denitrification process did not significantly increase the removal rate of NO_3^--N compared with 3#, which shows that the COD concentration in runoff rainwater is high. Under the high C/N, the COD in runoff rainwater can meet the demand of denitrification for carbon sources. Gilchrist et al., (Jiang et al., 2018) also found that the addition of wood chips did not significantly affect the removal rate of nitrate-nitrogen under conditions of sufficient carbon source. But the removal rate of NO_3^--N by the 1# bioretention cell was always low. The reason may be that the permeability coefficient of $1^{\#}$ is large. When the water infiltrated, the original anaerobic environment in the bioretention cell was destroyed, and denitrification was inhibited, resulting in short hydraulic retention time in the bioretention cell. Since the reaction rate of the nitrate-reducing bacteria in the denitrification process is greater than the reaction rate of the nitrite-reducing bacteria, the denitrification stays in the nitrate-reducing bacteria to convert NO_3^- into the NO_2^- phase in the case of short residence time, resulting in NO_2^- accumulation. Anaerobic ammonium oxidation (Anammox) (Hamilton, 2007) oxidizes the electron donor immobilized as an inorganic carbon source to NO_3^- under the action of anammox bacteria, resulting in a low NO_3^--N removal rate.

3.4. Effect of dry and wet alternation on the removal of dissolved N in each system

The bioretention cells often experience different rainfall events in practical application. Under the alternate operation of the wet and dry climate, it has been proved that the alternation of the wet and dry will cause the change of the soil structure and affect the pore size and stability of soil. Also, the alternation of dry and wet also affects the quantity and activity of microorganisms and the mineralization of organic matter. In order to study the effect of alternation of dry and wet on the experiment (Borken and Matzner, 2009), Different wet and dry alternating cycles were designed according to the interval of rainfall events in Xi'an, which were wet for 3 d, 3 d, 10 d and 5 d, and the dry periods were 5 d, 10 d and 5 d respectively during the wet period. The effects of dry-wet alternating on the removal of NH_4^+-N and NO_3^--N were investigated. The concentrations of NO_3^--N and NH_4^+-N in the inflow were 8.58 ± 0.22 and 8.65 ± 0.59 mg/L, respectively. The concentrations of NH_4^+-N and NO_3^--N in the effluent of each bioretention cell under the conditions of dry and wet alternate conditions are shown in Fig. 6(a). The concentration of NH_4^+-N in the effluent of each system in the wet period was not much different, and all were below 0.4 mg/L. The concentration of NH_4^+-N in each of the bioretention cells increased during the dry period. This is because the solute in the dry period and the dissolved microbial cells are released into the bioretention cell so that the available carbon source of the bioretention cell is increased and C is increased (Yun-Long et al., 2014). High C/N promotes the nitrate-nitrogen reduction process (DNR) in the submerged zone, producing NH_4^+-N (Saliling et al., 2007). Fowdar et al. (2015) also found that the increase in NH_4^+-N concentration is related to the NH_4^+-N produced by the DNRA process The removal rate of NH_4^+-N in the bioretention cell increased rapidly after the water in the wet period, because the height of the inundation area recovered to the previous level after immersion, and the anaerobic environment stimulated the action of denitrifying bacteria. The conversion, indirectly, led to an increase in nitrification, which caused the conversion of NH_4^+-N to the NO_3^--N direction. The influent of the bioretention cell after the dry period not only increased the oxygen content of the bioretention cell to promote nitrification but also washed away a large number of dead microorganisms and unfixed carbon sources. NO_3^--N was not easily reduced to NH_4^+-N when the bioretention cell formed a

Table 7
Concentration of dissolved nitrogen in effluent.

Saturation depth	NH_4^+-N (mg/L)			NO_3^-N (mg/L)		
	1#	2#	3#	1#	2#	3#
0 cm	0.46 ± 0.07	0.25 ± 0.06	0.35 ± 0.13	7.83 ± 0.46	5.26 ± 0.43	5.84 ± 0.54
300 cm	0.96 ± 0.13	0.20 ± 0.16	0.17 ± 0.09	7.40 ± 0.41	0.91 ± 0.37	0.52 ± 0.27
600 cm	0.10 ± 0.08	0.13 ± 0.09	0.12 ± 0.06	4.06 ± 0.49	0.14 ± 0.04	0.62 ± 1.06

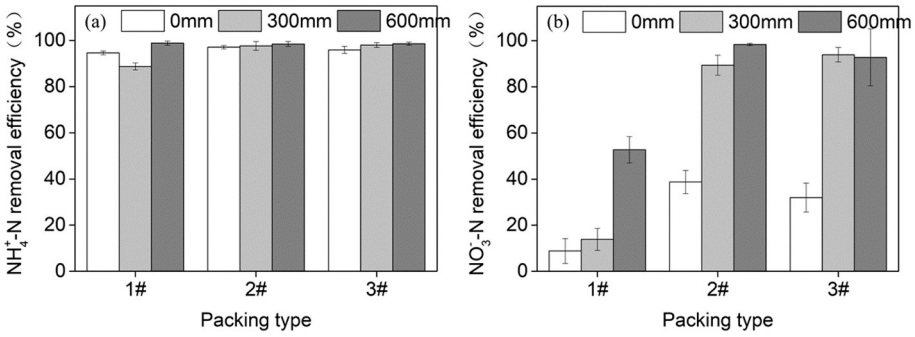

Fig. 5. Removal rate of (a) NH_4^+-N and (b) NO_3^--N at three submerged zone heights.

Table 8
The hydraulic retention time of the different height of the submerged zone in each bioretention cells.

Saturation depth	the hydraulic retention time		
	1#	2#	3#
0 cm	6 h	7 h	8 h
300 cm	9 h	10 h	12 h
600 cm	11 h	13 h	15 h

submerged zone, so NH_4^+-N caused the water concentration to gradually decrease until it stabilized.

It can be seen from Fig. 6(b) that the concentration of NO_3^--N in the effluent of each bioretention cell differs greatly during the wet period. In the fourth wet period, the bioretention cell 3# had the highest removal rate of NO_3^--N, followed by 2#, 1#, The average effluent concentration of three bioretention cells were 0.11 mg/L, 0.22 mg/L, and 3.09 mg/L, respectively. The results showed that the removal of NO_3^--N by concrete sand, loess or bioretention cell with concrete sand, loess, and sawdust as improved filler were better than other bioretention cells in the case of alternating wet and dry conditions. During the dry period of each bioretention cell, due to the long hydraulic retention time, most of the NO_3^--N in the bioretention cell was removed by denitrification, resulting in a decrease in the concentration of NO_3^--N. after entering the wet period, the concentration of NO_3^--N increased first and then decreased. One reason is that the evaporation of water during the dry period leads to a decrease in the submergence height, the death of a large number of microorganisms in the system, and the decrease in the activity of denitrifying bacteria. Another reason is the increase of NH_4^+-N in the system during the dry period. Anaerobic ammonium oxidation occurs under anaerobic conditions and produces NO_3^--N at the beginning of the wet period. After a few days in the wetting period, the denitrifying ability of the denitrifying bacteria gradually increased, resulting in a decrease in the NO_3^--N effluent concentration.

4. Conclusions

For the bioretention cells with collapsible loess as filler, the filling material is easy to collapse and block. Using construction waste, concrete sand and wood chips mixed with loess as the filler can not only effectively improve these shortcomings, improve the stability and permeability coefficient, but also ensure the pollutant removal rate. Based on changing the packing material, the operation effect of bioretention cells under the conditions of different submerged height and dry wet alternate circulation was studied. The conclusions are as follows: (1) the stability and permeability of the three improved fillers are significantly improved compared with loess fillers. (2) With the increase of hydraulic load, the removal rate of NO_3^--N decreased. But it has little effect on the removal rate of NH_4^+-N. The removal rate of NO_3^--N and NH_4^+-N was the highest. (3) When the submerged area was set at 600 mm, the removal rates of NO_3^--N and NH_4^+-N were higher, and the best treatment effect was obtained in 2#. (4) Under the condition of alternation of drying and wetting, the concentration of NH_4^+-N increased in the dry period and decreased in the wet period, which could be reduced to less than 0.4 mg/L. However, the difference of NO_3^--N was large, and the removal rates of 2# and 3# were the highest, and the difference was not significant.

Credit author statement

Jiaqing Xiong: Conceptualization; Formal analysis; Funding acquisition; Methodology; Writing - original draft; Writing - review & editing.
Jiajia Zhou: Data curation; Formal analysis; Investigation; Writing - review & editing.
Jianqiang Li: Formal analysis; Investigation; Software.
Guoqing Sun: Investigation.
Xiaochang C. Wang: Project administration; Resources; Supervision.
Shengxia An: Investigation; Validation.
Wanqin Li: Investigation; Validation.
Jie Wang: Investigation.

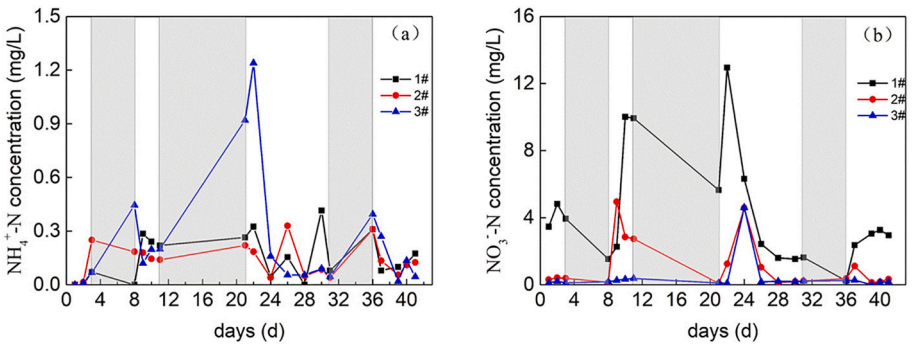

Fig. 6. (a) NH_4^+-N and (b) NO_3^--N effluent concentration (mg/L), 1# represents 50% construction waste, and 50% loess mixed filler, 2# represents 50% concrete sand, and 50% loess mixture The filler, 3# represents 45% concrete sand, 10% wood chips and 45% loess mixed filler. The area in the figure is shaded by gray to indicate the drying period, and no shade indicates the wet period.

Declaration of Competing Interest

None.

Acknowledgements

This work is supported by the National Program of Water Pollution Control (Grant No. 2012ZX07308-001-08).

References

Liu, Zhiwei, Shen, Rutao, 2009. Field tests on pre-bored compaction lime-soil pile (down-hole dynamic compaction method) to improve serious collapsible loess. Rock Soil Mech. 30, 339–343. https://doi.org/10.16285/j.rsm.2009.s2.075.

Liu, Zhen, Liu, Fengyin, Ma, Fuli, Wang, Mei, Bai, Xiaohong, Zheng, Yonglai, Yin, Hang, Zhang, G., 2015. Collapsibility, composition, and microstructure of loess in China. Can. Geotech. J. 53https://doi.org/10.1139/cgj-2015-0285. cgj-2015-0285.

Borken, Werner, Matzner, Egbert, 2009. Reappraisal of drying and wetting effects on C and N mineralization and fluxes in soils. Glob. Chang. Biol. 15, 808–824. https://doi.org/10.1111/j.1365-2486.2008.01681.x.

Anping, H., Yuming, S., 2019. Numerical simulation and analysis of flow in a variable waterhead reservoir in the presence of vortex. Electron. Measur. Technol. 42, 10–14. https://doi.org/10.19651/j.cnki.emt.1802077.

Davidson, E.A., Savage, K.E., Bettez, N.D., Marino, R., Howarth, R.W., 2009. Nitrogen in runoff from residential roads in a coastal area. Water Air Soil Pollut. 210, 3–13. https://doi.org/10.1007/s11270-009-0218-2.

Fan, G., Li, Z., Wang, S., Huang, K., Luo, J., 2019. Migration and transformation of nitrogen in bioretention system during rainfall runoff. Chemosphere 232, 54–62. https://doi.org/10.1016/j.chemosphere.2019.05.177.

Fowdar, H.S., Hatt, B.E., Breen, P., Cook, P.L., Deletic, A., 2015. Evaluation of sustainable electron donors for nitrate removal in different water media. Water Res. 85, 487–496. https://doi.org/10.1016/j.watres.2015.08.052.

Gao, Y., Jia, Y., Yu, G., He, N., Zhang, L., Zhu, B., Wang, Y., 2019. Anthropogenic reactive nitrogen deposition and associated nutrient limitation effect on gross primary productivity in inland water of China. J. Clean. Prod. 208, 530–540. https://doi.org/10.1016/j.jclepro.2018.10.137.

Hai-Zhen, M.I., Yang, Z.P., 2011. Experimental study on permeability of three kinds of improved loess. Build. Sci. 27, 41–43. https://doi.org/10.13614/j.cnki.11-1962/tu.2011.11.002.

Hamilton, B.S.K., 2007. Have we overemphasized the role of denitrification in aquatic ecosystems? A review of nitrate removal pathways. Front. Ecol. Environ. 5, 89–96 (doi:10.189011540-9295(2007)5[89,HWOTRO]).

Jiang, C.B., Li, J.K., Zhang, B.H., Ruan, T.S., Li, H.E., Dong, W., 2018. Design parameters and treatment efficiency of a retrofit bioretention system on runoff nitrogen removal. Environ. Sci. Pollut. Res. Int. 25, 33298–33308. https://doi.org/10.1007/s11356-018-3267-5.

Jing, C., Luo, M., Dong, B., 2014. Micro-mechanism of dynamic compaction on collapsible loess. J. Civil Architect. Environ. Eng. 36, 30–36. https://doi.org/10.11835/j.issn.1674-4764.2014.03.006.

Jinhui, L.I., Zhou, T., Zeng, C., Zhang, J., Hangfen, L.I., Zhao, Y., 2017. Removal of NH_4~+-N from aqueous solutions using foam concrete. Chin. J. Environ. Eng. 11, 4718–4724. https://doi.org/10.12030/j.cjee.201607189.

Kellogg, D.Q., Gold, A.J., Cox, S., Addy, K., August, P.V., 2010. A geospatial approach for assessing denitrification sinks within lower-order catchments. Ecol. Eng. 36, 1596–1606. https://doi.org/10.1016/j.ecoleng.2010.02.006.

LeFevre, G.H., Paus, K.H., Natarajan, P., Gulliver, J.S., Novak, P.J., Hozalski, R.M., 2015. Review of dissolved pollutants in urban storm water and their removal and fate in bioretention cells. J. Environ. Eng. 141. https://doi.org/10.1061/(ASCE)EE.1943-7870.0000876.

Mahmoud, A., Alam, T., Yeasir, A., Rahman, M., Sanchez, A., Guerrero, J., Jones, K.D., 2019. Evaluation of field-scale stormwater bioretention structure flow and pollutant load reductions in a semi-arid coastal climate. Ecol. Eng. https://doi.org/10.1016/j.ecoena.2019.100007.

O'Reilly, A.M., Chang, N.B., Wanielista, M.P., 2012. Cyclic biogeochemical processes and nitrogen fate beneath a subtropical stormwater infiltration basin. J. Contam. Hydrol. 133, 53–75. https://doi.org/10.1016/j.jconhyd.2012.03.005.

Peng, Y., Zhang, H., Lin, C., Wang, X., Yang, L., 2017. Engineering properties and improvement mechanism of loess soil modified by consolid system. Chin. J. Rock Mech. Eng. 36, 762–772. https://doi.org/10.13722/j.cnki.jrme.2015.1782.

Roberts, H.M., Muhs, D.R., Iii, E.A.B., 2013. Loess records | North America. Encycl. Q. Sci. 266, 620–628.

Sadeghi, H., Kiani, M., Sadeghi, M., Jafarzadeh, F., 2019. Geotechnical characterization and collapsibility of a natural dispersive loess. Eng. Geol. 250, 89–100. https://doi.org/10.1016/j.enggeo.2019.01,015.

Saliling, W.J.B., Westerman, P.W., Losordo, T.M., 2007. Wood chips and wheat straw as alternative biofilter media for denitrification reactors treating aquaculture and other wastewaters with high nitrate concentrations. Aquac. Eng. 37, 222–233. https://doi.org/10.1016/j.aquaeng.2007.06.003.

Shrestha, S., Bhatta, B., Shrestha, M., Shrestha, P.K., 2018. Integrated assessment of the climate and landuse change impact on hydrology and water quality in the Songkhram River Basin, Thailand. Sci. Total Environ. 643, 1610–1622. https://doi.org/10.1016/j.scitotenv.2018.06.306.

Tang, S., Luo, W., Jia, Z., Shan, L.I., Yan, W.U., Zhou, M., 2016. Effects of filler and rainfall characteristics on runoff reduction of rain garden and achieving the goal of sponge city construction. J. Soil Water Conserv. 30, 73–78. https://doi.org/10.13870/j.cnki,stbcxb.2016.01.015.

Tian, J., Jin, J., Chiu, P.C., Cha, D.K., Guo, M., Imhoff, P.T., 2019. A pilot-scale, bi-layer bioretention system with biochar and zero-valent iron for enhanced nitrate removal from stormwater. Water Res. 148, 378–387. https://doi.org/10.1016/j.watres.2018.10.030.

Wang, H.W., Zhai, Y.J., Wei, Y.Y., Mao, Y.F., 2019. Evaluation of the effects of low-impact development practices under different rainy types: case of Fuxing Island Park, Shanghai, China. Environ. Sci. Pollut. Res. Int. 26, 6706–6716. https://doi.org/10.1007/s11356-019-04129-X.

Wan-Li, Xie, Yan-Shou, Wang, Yan-Shou, Wang, Rui-Hua, Ge, Rui-Hua, Ge, 2015. Research status and prospect of loess collapsibility mechanism. Geoscience 29, 397–407.

Wei, C.J., Wei-Zhong, W.U., Tao, S., De-Sheng, L.I., 2010. Multi-soil-layer system for treatment of polluted river water flowing into Dianchi Lake. Chin. Water Wastewater 26, 104–106. https://doi.org/10.19853/j.zgjsps.1000-4602.2010.09.028.

Yun-Long, H.E., Yu-Chun, Q.I., Dong, Y.S., Qin, P., Sun, L.J., Jia, J.Q., Guo, S.F., Yan, Z.Q., 2014. Microbial response mechanism for drying and rewetting effect on soil respiration in grassland ecosystem: a review. Chin. J. Appl. Ecol. 25, 3373–3380.

Zhang, W., Sun, Y., Chen, W., Song, Y., Zhang, J., 2019. Collapsibility, composition, and microfabric of the coastal zone loess around the Bohai Sea, China. Eng. Geol. 257. https://doi.org/10.1016/j.enggeo.2019.05.019.

Zheng-Zheng, L.I., Gao, X.W., 2018. Study on collapsibility of remolded loess by model test and evaluation of loess collapsibility. Sci. Technol. Eng. 18, 319–327.

Zhirong, Wu., 2019. The mechanism of collapsible loess foundation and its treatment are discussed. Shanxi Architect. 45, 64–65. https://doi.org/10.13719/j.cnki.cn14-1279/tu.2019.01.036.